Biogeosciences, 9, 2301–2309, 2012
www.biogeosciences.net/9/2301/2012/
doi:10.5194/bg-9-2301-2012

Biogeosciences

Direct observations of diel biological CO_2 fixation on the Scotian Shelf, northwestern Atlantic Ocean

H. Thomas[1], S. E. Craig[1], B. J. W. Greenan[2], W. Burt[1], G. J. Herndl[3,4], S. Higginson[1], L. Salt[4], E. H. Shadwick[1,5], and J. Urrego-Blanco[1]

[1]Dalhousie University, Department of Oceanography, Halifax, NS, Canada
[2]Bedford Institute of Oceanography, Fisheries & Oceans Canada, Dartmouth, NS, Canada
[3]University of Vienna, Department of Marine Biology, Vienna, Austria
[4]Royal Netherlands Institute for Sea Research, Department of Biological Oceanography, Texel, The Netherlands
[5]Antarctic Climate & Ecosystems Cooperative Research Centre, University of Tasmania, Hobart, Tasmania, Australia

Correspondence to: H. Thomas (helmuth.thomas@dal.ca)

Received: 10 February 2012 – Published in Biogeosciences Discuss.: 24 February 2012
Revised: 2 June 2012 – Accepted: 5 June 2012 – Published: 27 June 2012

Abstract. Much of the variability in the surface ocean's carbon cycle can be attributed to the availability of sunlight, triggering surface heat flux and photosynthesis, which in turn regulate the biogeochemical cycling of carbon over a wide range of time scales. The critical processes of this carbon cycle regulation, occurring at time scales of a day or less, however, have undergone few investigations, most of which have been limited to time spans of several days to months. Optical methods have helped to infer short-term biological variability, but complementing investigations of the oceanic CO_2 system are lacking. We employ high-frequency CO_2 and optical observations covering the full seasonal cycle on the Scotian Shelf, northwestern Atlantic Ocean, in order to unravel diel periodicity of the surface ocean carbon cycle and its effects on annual budgets. Significant diel periodicity in the surface CO_2 system occurs only if the water column is sufficiently stable as observed during seasonal warming. During that time biological CO_2 drawdown, or net community production (NCP), is delayed for several hours relative to the onset of photosynthetically available radiation (PAR), due to diel cycles in chlorophyll *a* concentration and to grazing. In summer, NCP decreases by more than 90 %, coinciding with the seasonal minimum of the mixed layer depth and resulting in the disappearance of the diel CO_2 periodicity in the surface waters.

1 Introduction

Shelf and marginal seas play a crucial role in the global carbon cycle as they link terrestrial, marine and atmospheric compartments (Ciais et al., 2008; Thomas et al., 2008; Chen and Borges, 2009). As a consequence of their role as an integral link between the compartments, the spatial and temporal variability of the carbon cycle in marginal seas is generally higher than in open ocean environments (Thomas and Schneider, 1999; Schiettecatte, 2006; Chen and Borges, 2009; Omar et al., 2010). In addition to natural drivers, anthropogenic processes perturbing natural cycles in each of the carbon cycle compartments affect variability in shelf and marginal seas. Examples of such perturbations include eutrophication, ocean acidification and atmospheric nitrogen deposition (Doney et al., 2007; Thomas et al., 2009; Borges and Gypens, 2010; Cai et al., 2011).

Physical, biological and chemical processes govern the variability of the carbon cycle and the air-sea exchange of CO_2. Although these processes are evident at many temporal and spatial scales, they interact at high frequency local scales, eventually yielding diurnal, seasonal and longer-term periodicity. Our understanding of the monthly to seasonal variability in the carbon cycle in several shelf and marginal seas has improved, in particular with respect to attaining full annual observational coverage (Chen and Borges, 2009; Omar et al., 2010; Thomas et al., 2004; Shadwick et al., 2010, 2011a). At shorter time scales, optical methods have helped to infer

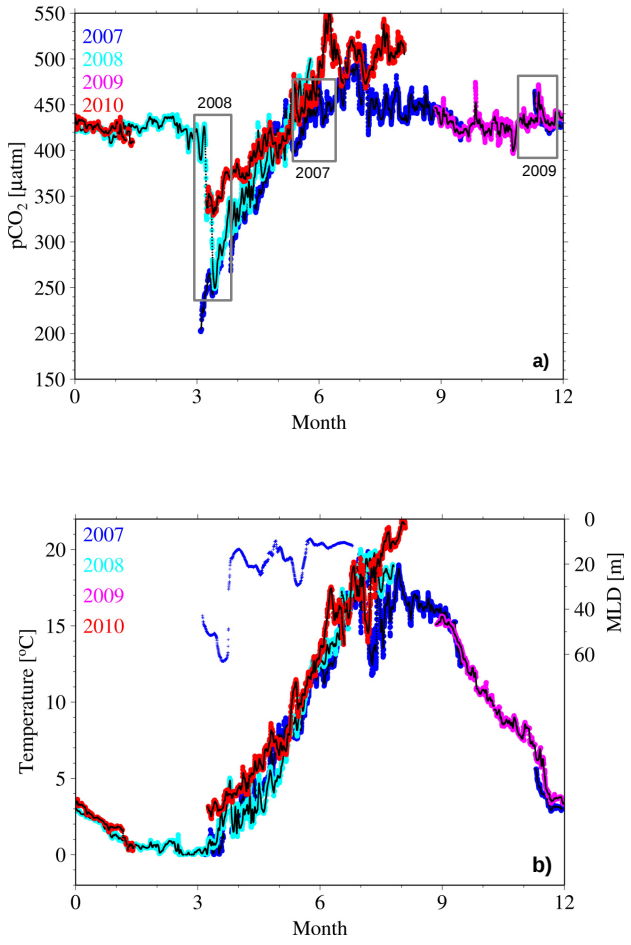

Fig. 1. Composite of available pCO_2 **(a)** and temperature data **(b)** for the years 2007–2010, recorded by the CARIOCA buoy. For the further study we evaluate data from June/July 2007, April 2008 and November/December 2009 as indicated by the grey boxes in **(a)**, assuming a climatological annual cycle. The black lines indicate the 48-point moving average. In **(b)**, the depth of the maximum of the Brunt-Väisälä frequency is shown as measure of the mixed layer depth (MLD, blue crosses), computed from the SeaHorse data, deployed between April 2007 and July 2007.

short-term biological variability (Siegel et al., 1989; Stramska and Dickey, 1992; Cullen et al., 1992; Gernez et al., 2011; Dall'Olmo et al., 2011). However, corresponding investigations of the oceanic CO_2 system are largely lacking. A few recent studies have focused on time scales of several days to months (Hood et al., 2001; Bates et al., 2001; Copin-Montegut et al., 2004; Lefèvre et al., 2008; Boutin and Merlivat, 2009; Leinweber et al., 2009; Bozec et al., 2011; Lefèvre and Merlivat, 2012). Investigations of processes at the rate of their occurrence in shelf and marginal seas are still sparse when it comes to full seasonal coverage (Vandemark et al., 2011).

The Scotian Shelf region is located at the eastern Canadian continental shelf at the boundary between the subpolar and subtropical gyres. This region is thus influenced by water masses of Arctic origin via the Labrador and Newfoundland Shelves, by low-salinity waters emanating from the Gulf of St. Lawrence, and by the Gulf Stream (Urrego-Blanco and Sheng, 2012). One of the dominant characteristics on the shelf is the large seasonal amplitude in sea surface temperature (SST) between subzero temperatures in winter to approximately 20 °C during summer (Shadwick and Thomas, 2011) (Fig. 1). Recent studies have identified this region as a strong source for atmospheric CO_2 at the annual scale, with an intense, but brief period of CO_2 uptake during the spring bloom, which occurs at the annual SST minimum in late March to early April (Shadwick et al., 2011a) (Fig. 1). Controls of the seasonal to interannual variability of the surface CO_2 system in the Scotian Shelf region have been inferred from satellite observations, and include the intensity of autumn and winter storms, winter nutrient levels, and the onset of post-winter water column stratification (Greenan et al., 2004, 2008; Shadwick et al., 2010). The processes controlling the variability of the carbon cycle at time scales shorter than the monthly to seasonal scale remain poorly understood, which is the case for most regions of the open oceans, as well as for shelf and marginal seas. This study sheds light on the role of high frequency processes in controlling the carbon cycle in the surface waters of the Scotian Shelf region over a complete annual cycle. In particular, we investigate the occurrence of processes with diel periodicity, how their occurrence is controlled and how they contribute to seasonal and annual patterns of the surface water CO_2 system on the Scotian Shelf.

2 Material and methods

Investigations of the carbon cycle on the Scotian Shelf were initiated in 2006, and comprise shipboard observations of the carbon cycle and complementary parameters through the entire water column, as well as deployment of a CARIOCA buoy. Sporadically, these observations were paralleled by the deployment of the SeaHorse profiler, as detailed below. In-depth descriptions of the buoy location and the corresponding sampling activities have been given in Shadwick et al. (2011a). Here, we employ observations from the CARIOCA buoy, deployed since April 2007, that records surface water pCO_2, SST, salinity, and complementary parameters at an hourly rate and at a depth of approximately 2 m. Details of the CARIOCA sensor have been reported for example by Bates et al. (2000, 2001), Bakker et al. (2001) and Hood and Merlivat (2001). In order to avoid data gaps due to maintenance, we reconstruct an annual cycle using different years of observations (Fig. 1). We focus on three key periods of the annual cycle: firstly, winter (pre-spring bloom to spring bloom transition); secondly, late spring to early summer, i.e. the warming period; and thirdly, the autumn to winter transition (Fig. 1). Diel cycles in pCO_2 with hourly resolution

were established by removing the 48-point moving average from the (hourly) observations, which is similar to the approach pursued by Leinweber et al. (2009). We corrected the in-situ pCO_2 observations ($pCO_{2,\,obs}$) for each day to the daily mean temperature ($pCO_{2,\,temp}$) of that day using the full suite of carbonate system equations via the CO2SYS program (Lewis and Wallace, 1998) with the constants by Dickson and Millero (1987). As discussed in Sect. 3, the difference between these values reveals the biologically driven change of pCO_2 ($pCO_{2,\,bio}$):

$$pCO_{2,\,obs} - pCO_{2,\,temp} = pCO_{2,\,bio}\,. \quad (1)$$

Mean diel cycles for the spring period (days 160–200 representing the period, when surface waters warm) were computed as the corresponding 40-day average of each hour of the day (Figs. 2a, b, 4d). Under consideration of the salinity records of the CARIOCA buoy and the salinity-alkalinity relationship reported by Shadwick et al. (2011a), we computed dissolved inorganic carbon (DIC) concentrations as a function of pCO_2 and alkalinity using CO2SYS (Lewis and Wallace, 1998) and the carbonate system constants by Dickson and Millero (1987). The integration of the biological component of the diel DIC cycles yielded the estimates of the biological rates.

In order to investigate the crucial period between spring and summer, when the waters are warming (Fig. 1), we combined the CARIOCA data with observations from the SeaHorse, an autonomous profiler (Greenan et al., 2004, 2008), which records water column profiles of temperature, salinity, photosynthetically available radiation (PAR), and downwelling irradiance ($E_d(\lambda)$) between 3–80 m depth. Profiles were recorded with approximately 0.5 m vertical resolution approximately every 2 h between 4 April 2007 and 27 July 2007. The comparison of the diel temperature anomaly recorded at the sea surface by the CARIOCA buoy and the SeaHorse, respectively, shows good agreement of both instruments in timing and amplitude (Fig. 2a). The obtained diel cycle in surface temperature with an amplitude of 0.2–0.3 °C is the result of incoming solar radiation of approximately 500 W m^{-2} over 10–12 h per day in a mixed layer depth (MLD) of 10–20 m.

In an attempt to resolve the contribution of phytoplankton to NCP during the warming period, we derived chlorophyll *a* concentrations between 5 and 6 m from profiles of SeaHorse $E_d(\lambda)$ using the model of Nahorniak et al. (2001). This depth range was chosen to be as close to the depth of the CARIOCA sensors (2 m) as possible, whilst preventing the inclusion of noisy E_d data due to surface light wave focusing. The model required that the attenuation of E_d is calculated at three wavelengths (412, 443, 555 nm) over a depth interval (5–6 m). Since the sensor wavelengths (379.3, 442.9, and 491 nm) did not exactly match the wavelengths required by the model, $E_d(\lambda)$ was first interpolated to model wavelengths. Modelled chlorophyll *a* (Chl_{mod}; mg m^{-3}) at an average depth of 5.5 m (i.e. half way between 5 and 6 m)

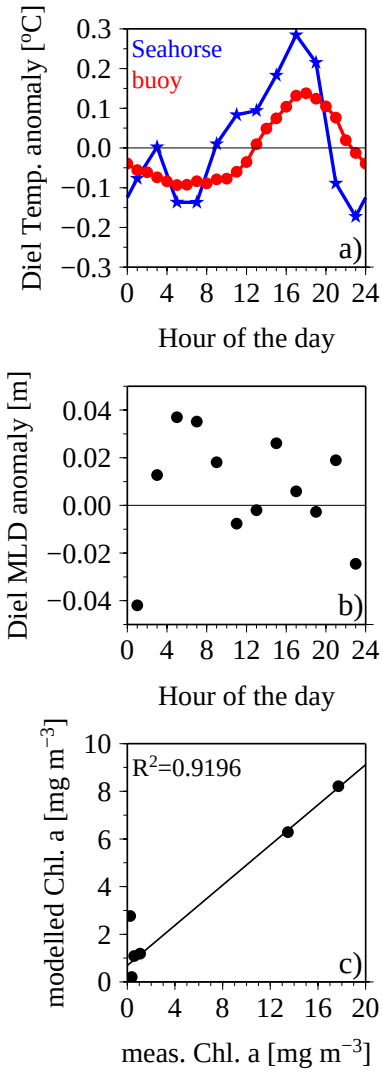

Fig. 2. (a) Comparison of the diel temperature anomaly recorded by the CARIOCA buoy (red) and the SeaHorse profiler (blue), shown as average of the days 160–200. **(b)** Diel MLD anomaly, shown as average of the days 160–200, computed from the maximum of the Brunt-Väisälä frequency as measure of the MLD. **(c)** Correlation between the Chl *a* concentrations measured and modelled after Nahorniak et al. (2001).

was then calculated using Nahorniak et al.'s (2001) formulations that include spectral coefficients to describe the absorption properties of water, phytoplankton and coloured dissolved organic matter and assume a value of 0.8 for the average cosine of downwelling light, μ_d (dimensionless). Chl_{mod} values were compared with discrete, fluorometrically determined chlorophyll *a* values obtained at the same time and depth from ship-based water samples (Fig. 2c), and R^2, root mean square error (RMSE; mg m^{-3}) and bias (mg m^{-3}) values of 0.92, 4.31 mg m^{-3}, and −1.76 mg m^{-3} ($N = 8$), respectively, were obtained. These values were then grouped into periods 1–3 as described above, and averaged into time

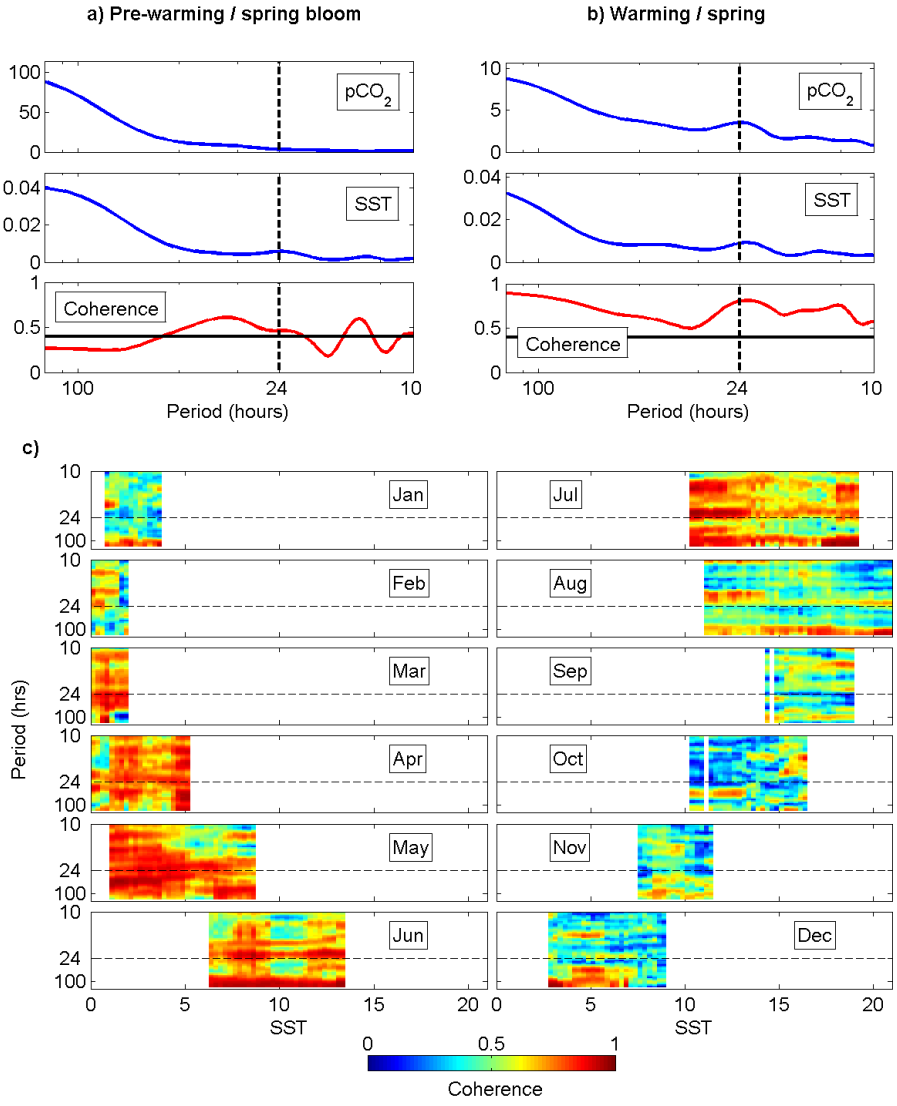

Fig. 3. Spectral analysis of pCO_2 and SST data from the CARIOCA buoy. Power spectra of pCO_2 and SST and their coherence are shown for two periods: **(a)** the pre-warming/spring bloom period and **(b)** the warming period (see Fig. 1a grey boxes). The dashed line on each plot indicates the 24 h period, and the horizontal solid line on the coherence plots shows the 5 % significance level based on the degrees of freedom of the cross-spectral estimators. The coherence between pCO_2 and SST is plotted as a function of SST in monthly composites **(c)**, illustrating the temporal evolution of the coherence. The colour scale indicates the level of coherence between pCO_2 and SST, and the dashed line shows the 24 h period. High coherence at the 24 h period occurs only when the water is warming.

bins to give climatological values for Chl_{mod} every two hours during the hours of daylight when reliable $E_d(\lambda)$ measurements could be made, which, at this time of year and latitude, corresponded to times between ~06:00–16:00 local time.

3 Results and discussion

The spectral analysis of the buoy data (Fig. 3a, b) revealed a 24-h periodicity for the parameters pCO_2 and SST that occurs only when the waters are warming, i.e. between April and late August. pCO_2 and SST also showed significant coherent patterns during this time of the year (Fig. 3b, bottom panel, Fig. 3c) and are the focus of this paper. Outside of this period, periodicity and significant coherence were only observed, if detected, at longer time scales (several days), which mirrors the typical frequency of winter storms in the region (Fig. 3c). Other parameters, such as salinity, do not show significant 24-h periodicity, which means that tidal, lateral and other effects are either not identifiable, or act on timescales longer than 24 h. Such processes would be captured by the 48-point moving average and do not influence the diel cycles. We also verified the potential role of daily cycles in MLD, which could lead to an intrusion of CO_2-rich

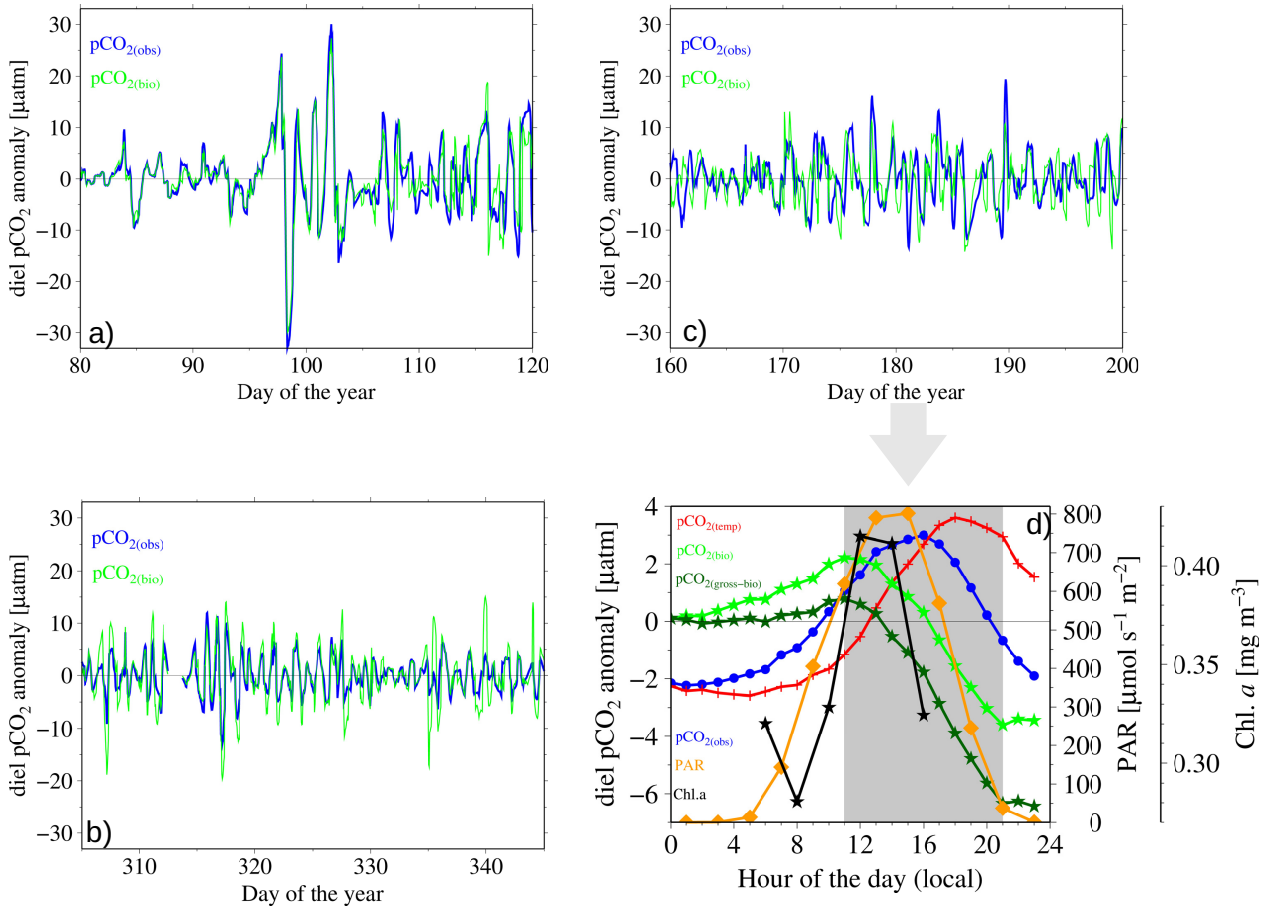

Fig. 4. Diel anomalies and daily cycles of observed pCO_2, biologically controlled pCO_2, PAR, and Chl *a*. We show diel anomalies of $pCO_{2,\,obs}$ (blue) and $pCO_{2,\,bio}$ (green) for three periods of the year (**a**–**c**) as depicted in Fig. 1. Note the phase shift in the warming period (**c**, **d**), while outside the warming period (**a**, **b**) both parameters show the same timing (i.e. they are independent). Average diel anomalies or daily cycles compiled for the 40-day period from days 160–200, representative for the warming period (see Fig. 1), for observed pCO_2 ($pCO_{2,\,obs}$, blue), biologically controlled pCO_2 ($pCO_{2,\,bio}$, green), temperature-only controlled pCO_2 ($pCO_{2,\,temp}$, red), $pCO_{2,\,bio}$ corrected for respiratory activity ($pCO_{2,\,gross\text{-}bio}$, dark green) and photosynthetic active radiation (PAR, orange). Chlorophyll *a* (Chl *a*, black) is shown for the hours (6.00 h–16.00 h), when reliable $E_d(\lambda)$ measurements can be made by the SeaHorse. The grey-shaded box indicated the period, when net carbon fixation occurs. Note that $pCO_{2,\,temp}$ reflects the daily cycle of temperature. The respiration rate has been computed from the slope of the $pCO_{2,\,bio}$ during nighttime conditions. The production rates have been computed from the slopes of $pCO_{2,\,bio}$ and $pCO_{2,\,gross\text{-}bio}$ during daytime (grey-shaded area), respectively. The time scale reveals local time, i.e. GMT − 3 h.

water into the surface layer, if the MLD deepens. Boutin and Merlivat (2009) suggested that this process is an important driver of the diel pCO_2 anomaly. Leinweber et al. (2009), however, suggest that the deepening of the MLD is of minor importance due to the absence of a strong vertical gradient in DIC at their study site. The computation of the diel MLD anomaly for our location did not reveal a significant diel pattern, with variability, on the order of a few tens of centimeters (Fig. 2b), given a MLD of 10–20 m. We therefore consider the influence of temperature-driven diel variability in MLD as negligible in our case. CO_2 air-sea fluxes play a very minor role on the surface layer DIC concentrations at the 24 h time scale, such that the feedback between pCO_2 and CO_2 air-sea fluxes is negligible in our study.

Surface heat fluxes cause variability in SST at diel and seasonal time scales (Umoh and Thompson, 1994), which in turn drive some of the observed variability of the pCO_2, primarily because of the temperature dependence of the Henry constant. We corrected the observed pCO_2 data ($pCO_{2,\,obs}$) to a daily mean temperature to give $pCO_{2,\,temp}$. The difference between $pCO_{2,\,obs}$ and $pCO_{2,\,temp}$ yielded pCO_2 data that were governed by processes other than temperature within a 24-h period. Since we did not detect processes other than SST variability acting on the 24 h period, the remaining pCO_2 variability was ascribed to biological activity ($pCO_{2,\,bio}$, Eq. 1). The daily and diel variability of the $pCO_{2,\,obs}$ and $pCO_{2,\,bio}$ for three periods of the year is shown in Fig. 4. In the winter period (days 80–95, Fig. 4a),

the amplitude of the diel oscillation was small and the pCO_2 relatively constant. With the onset of the spring bloom, at approximately day 95 (see also Shadwick et al., 2011a, their Figs. 4 and 16), the diel amplitude drastically increased (Fig. 4a). Throughout both of these periods, $pCO_{2,\,obs}$ and $pCO_{2,\,bio}$ were in phase and tracked each other closely indicating that temperature was not the main driver for the short-term variability during this time of the year. Similarly, in the autumn to winter (Fig. 4b) transition, $pCO_{2,\,obs}$ and $pCO_{2,\,bio}$ again revealed in-phase patterns, though with a higher amplitude in autumn (days 305–345) than in winter (days 80–95), which can be ascribed to deepening of the mixed layer and an intrusion of high pCO_2 subsurface waters into the surface mixed layer (Shadwick et al., 2011a). Between the days 160–200 (end of June until end of July), i.e. later in the season of surface water warming, the amplitude of the diel oscillation was reduced compared to that observed during the spring bloom (Fig. 4a–c). More importantly, a phase shift was detectable between $pCO_{2,\,obs}$ and $pCO_{2,\,bio}$, with the latter occurring approximately 3 h earlier than the $pCO_{2,\,obs}$ (Fig. 4c, d). We postulate that the cause for this phase shift might be diel cycles in biological activity. Such diel cycles were only visible, when the water column was sufficiently stable, such as during thermal stratification (Fig. 1b; Shadwick et al., 2011a, their Fig. 9). Outside the warming period, several processes have the potential to obscure or prevent diel signals or their detection: For example, during the autumn and winter periods, thermal stratification breaks down due to cooling air temperatures and increased wind-driven mixing resulting in a deepening of the mixed layer and greatly decreased photosynthetic activity, meaning that the diel cycles easily detectable during the warming period are difficult to detect or are completely absent in autumn and winter.

We can consider the diel cycle of pCO_2 as a composite of a temperature-driven component, which follows the diel cycle of SST (Fig. 4d), and a biologically driven component, controlled by the balance of production and respiration of organic matter. The diel biological cycle obtained here can be considered a net biological signal, which shows an increase of the $pCO_{2,\,bio}$, i.e. net respiration, beginning in the evening (approx. 21:00 h) and ending in the morning hours (10:00 h–11:00 h), when net community production (NCP) begins to exceed community respiration. NCP, indicated by a negative slope in the pCO_2 anomaly (Fig. 4d), dominates the system until dusk. Subtracting the respiration signal, computed from the slope of the $pCO_{2(bio)}$ during nighttime conditions, allows us to estimate the diurnal cycle of gross primary production (GPP). The corresponding respiration rate, assumed to be constant throughout the day, is estimated to be 0.05 µmol C $(l\,h)^{-1}$; the rates of NCP and GPP are 0.26 µmol C $(l\,h)^{-1}$ and 0.31 µmol C $(l\,h)^{-1}$, respectively, both lasting approximately 10 h per day. This compares well with the GPP estimates given by Forget et al. (2007, their Table 2), which, when combined with an assumed 30 m MLD, yield GPP rates of 13 µmol C $(l\,d)^{-1}$. It must be noted, however, that their station is somewhat further offshore at the shelf break than the mooring location of the CARIOCA buoy and the SeaHorse. Somewhat more difficult to compare are the daily production rates reported by Boutin and Merlivat (2009), which range between 1.8 µmol C $(l\,d)^{-1}$ and 4.8 µmol C $(l\,d)^{-1}$. While their method of estimating NCP is similar to our approach, the data were obtained in the Southern Ocean at comparable latitude, but from a drifting instrument.

The onset of the net photosynthetic CO_2 drawdown occurred approximately 4–5 h after sunrise, near the period maximum of PAR (Fig. 4d) – a phenomenon that has been frequently documented, but surprisingly has rarely been discussed or addressed in detail. Stramska and Dickey (1992), Siegel et al. (1989) and Gernez et al. (2011) report a phase shift of several hours between the onset of PAR and maximum values of either the beam attenuation coefficient (c_p) or dissolved oxygen (O_2) concentrations. The latter two are mirroring the build-up of photosynthetic organic matter and reveal phasing throughout the diurnal cycle, which is comparable to the phasing of $pCO_{2,\,bio}$. Bozec et al. (2011, their Fig. 5) also show a similar phase shift between dissolved O_2 and pCO_2, relative to PAR. They conclude, however, that pCO_2 and PAR are out of phase by 180 degree and O_2 is in phase with PAR. Leinweber et al. (2009) report similar but shorter time lags between their pCO_2 parameters, which tend to reveal stronger diel amplitudes than we observed. Overall, it appears that the temperature control of their system is more pronounced than on the Scotian Self, as evident from the higher diel temperature amplitude of 4 °C in the Santa Monica Bay (Leinweber et al., 2009), compared to 0.2 °C on the Scotian Shelf (Fig. 2a). Lefèvre and Merlivat (2012) report for the tropical eastern Atlantic a time lag between PAR and SST; however, the relationship with chemical parameters (DIC, oxygen) appears complex and variable, likely because of physical processes. In summary, it appears that there is sufficient evidence in the literature to suggest that the signal of net biological carbon fixation in the water column, as revealed by pCO_2, O_2, or beam attenuation measurements, is detectable at or around peak PAR, which is the ultimate energy source for the biological carbon fixation.

In order to determine whether this reported periodicity in metrics of phytoplankton photosynthetic activity occurred at our study site, we binned averaged Chl_{mod} over the 40-day warming period (days 160–200). This revealed a diel cycle with a difference of approximately 30 % (0.13 mg Chl $a\,m^{-3}$) between minimum and maximum values, with the lowest values corresponding to low PAR levels during early morning and late afternoon, and maximum values to peak PAR at around noon (Fig. 4d). Please note that the daily Chl_{mod} excursion is small compared to the RMSE of 4.31 mg m^{-3} (Fig. 2c), indicating that quantitative interpretation of Chl_{mod} results should be made with caution. However, even if not a truly quantitative estimate of Chl *a*, the diel, i.e. relative Chl_{mod} pattern, observed at our study site is

significant and, furthermore, is very similar to those observed in other studies of optical signals that have been interpreted as the combined effects of processes including daily primary production, phytoplankton sinking, and zooplankton grazing (Gardner et al., 1993; Marra, 1997; Stramska and Dickey, 1992; Gernez et al., 2011). When compared with the pCO_2 diel cycles, it was observed that the onset of net CO_2 drawdown, indicated by the change in slope of $pCO_{2,\,bio}$ from positive to negative, coincided with the time of the maximum Chl_{mod} values (Fig. 4d). In other words, our data suggest that a threshold Chl *a* concentration must first be attained during the growth phase before the system achieves net CO_2 drawdown. Others have also reported diel signals in either Chl *a* or photosynthetic parameters (Cullen et al., 1992; Bruyant et al., 2005), with peak values around noon. It should also be noted that photoinhibition may depress the photosynthetic rate at high irradiances, especially around noon, potentially further modulating the exact occurrence of net CO_2 drawdown with respect to PAR levels. Another process that may have contributed to the patterns in Chl_{mod} is phytoplankton diel vertical migration, whereby cells migrate to well lit surface waters during daylight hours and to deeper, nutrient rich waters at night. At this time of year (June–July), the phytoplankton community was dominated by flagellates (Harrison et al., 2008), which are well known to exhibit diel vertical migration patterns (Eppley et al., 1968; MacIntyre et al., 1997; Hall and Paerl, 2011), making it likely that this process contributed, at least in part, to both the accumulation of biomass during daylight hours and to the lag time between PAR and NCP, when the flagellates first have to move upward to reach the well lit surface during the early morning hours.

Both our results and those reported in the literature are consistent with the notion of a phase shift between the onset of PAR at dawn and of net carbon fixation at approximately solar noon. Meso- and microzooplankton, which are active during nighttime, might still exert grazing pressure on phytoplankton during the early morning hours and thereby keep the abundance of phytoplankton low during the initial hours of daylight (Siegel et al., 1989). In addition to grazing effects, the diurnal variability in phytoplankton photosynthetic activity itself also contributes to delaying net carbon fixation until PAR has reached approximately maximum values as discussed above. Furthermore, in order to detect net carbon fixation as a change in the pCO_2 (or O_2 concentrations) in the water column, primary producers have to compensate for the respiratory activity of the heterotrophs, which in turn might exhibit relatively constant activity rates throughout the diel cycle (Cullen et al., 1992; Gernez et al., 2011). Based on our analysis, we suggest that grazing and the dependence of the photosynthetic rate on PAR lead to a net-autotrophic system just before, or at, maximum PAR values (Fig. 4d). As mentioned earlier, in our study we were not able to identify any diurnal variability in the water column structure, i.e. in strength and depth of stratification, which might have provoked the phase shift between PAR and $pCO_{2,\,bio}$.

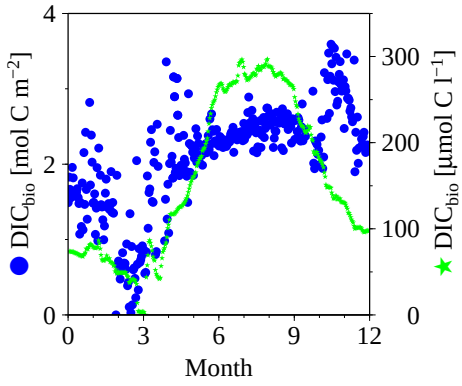

Fig. 5. Annual cycle of biological DIC uptake. We show the annual cycle of biological DIC uptake, integrated from hourly values, i.e. accumulated diel changes. The mixed layer inventory of biological DIC uptake (left y-axis, blue) was obtained by dividing the biological DIC concentration change (right y-axis, green) by the MLD as reported by Shadwick et al. (2011a).The production rates were computed from the slopes of the DIC uptake.

We have revealed the seasonal dynamics of NCP by integrating the hourly $pCO_{2,\,bio}$ values (Fig. 5), yielding the biologically driven DIC concentration change, or under consideration of the MLD, the NCP inventory. The maximum value of NCP is 3.4 mol C m^{-2} or 271 µmol C l^{-1}, which is with respect to temporal evolution and magnitude of NCP similar to the results reported by Shadwick et al. (2011a), thus underpinning the importance of biological processes in the surface layer DIC variability. This integration of hourly values provides further evidence for the ongoing biological CO_2 fixation after the spring bloom as a significant contributor to annual CO_2 fixation (Shadwick et al., 2011a, b). Of particular interest is the observation that the carbon fixation rate, i.e. the DIC uptake rate by phytoplankton, is fairly constant from the onset of the spring bloom (approx. day 100) to approximately day 180, with DIC uptake rates of approximately 2.5 µmol C (l d)$^{-1}$, corresponding to a NCP rate of 0.26 µmol C (l h)$^{-1}$, assuming a 10-h photoperiod per day (Fig. 4d). Again, this compares well with the GPP rates of 1–3 µmol C (l d)$^{-1}$ as reported by Forget et al. (2007) for this period. Charette et al. (2001) reported ^{14}C-based GPP rates, determined for the area in September 1997, of 0.9–13 µmol C (l d)$^{-1}$, assuming a 30 m MLD. These GPP rates were given without estimates of water column respiration, hindering a direct comparison to our data. The production rate decreases to about 0.1 µmol C (l d)$^{-1}$ (Fig. 5), when the mixed layer depth reaches its minimum. Thereafter, a combination of dramatically reduced availability of nutrients and photoinhibition of photosynthesis reduces NCP substantially in autumn.

4 Conclusions

In summary, we observed a statistically significant diurnal periodicity of the CO_2 system in surface waters only during the period when the water is warming. The corresponding increase in water column stability during warming facilitates the appearance of the diurnal cycle. The unravelled diurnal cycles of the surface pCO_2 reveal that net photosynthetic carbon fixation, i.e. NCP, begins approximately 4–5 h after onset of PAR. Grazing and transitional metabolic rates are likely the responsible processes for this phase shift, eventually allowing the ecosystem to be autotrophic for approximately 10 h out of 16 h of daylight during spring and early summer.

Acknowledgements. We gratefully acknowledge support from the Canadian Foundation for Climate and Atmospheric Sciences (CFCAS), the National Science and Engineering Research Council (NSERC), Metocean Datasystems. HT holds a Canada Research Chair for Marine Biogeochemistry. We would like to thank the DFO Atlantic Zone Monitoring Program (AZMP) for supporting the deployment and recovery of the moorings. We would also like to thank Rick Boyce, Jay Barthelotte and Jason Burtch for their assistance in the field operations. The paper greatly benefited from the comments by two anonymous referees. This work is a contribution to the IGBP/IHDP core project LOICZ.

Edited by: C. Heinze

References

Bakker, D. C. E., Etcheto, J., Boutin, J., and Merlivat, L.: Variability of surface water fCO_2 during seasonal upwelling in the equatorial Atlantic Ocean as observed by a drifting buoy, J. Geophys. Res., 106, 9241–9253, 2001.

Bates, N. R., Merlivat, L., Beaumont, L., and Pequignet, A. C.: Intercomparison of shipboard and moored CARIOCA buoy seawater fCO_2 measurements in the Sargasso Sea, Mar. Chem., 72, 239–255, 2000.

Bates, N. R., Samuels, L., and Merlivat, L.: Biogeochemical and physical factors in?uencing seawater fCO_2 and air-sea CO_2 exchange on the Bermuda coral reef, Limnol. Oceanogr., 46, 833–846, 2001.

Borges, A. V. and Gypens, N.: Carbonate chemistry in the coastal zone responds more strongly to eutrophication than to ocean acidification, Limnol. Oceanogr., 55, 346–353, 2010.

Boutin, J. and Merlivat, L.: New in situ estimates of carbon biological production rates in the Southern Ocean from CARIOCA drifter measurements, Geophys. Res. Lett., 36, L13608, doi:10.1029/2009GL038307, 2009.

Bozec, Y., Merlivat, L., Baudoux, A.-C., Beaumont, L., Blain, S., Bucciarelli, E., Danguy, T., Grossteffan, E., Guillot, A., Guillou, J., Répécaud, M., and Tréguer, P.: Diurnal to inter-annual dynamics of pCO_2 recorded by a CARIOCA sensor in a temperate coastal ecosystem (2003–2009), Mar. Chem., 126, 13–26, 2011.

Bruyant, F., Babin, M., Genty, B., Prasil, O., Behrenfeld, M. J., Claustre, H., Bricaud, A., Garczarek, L., Holtzendorff, J., Koblizek, M., Dousova, H., and Partensky, F.: Diel variations in the photosynthetic parameters of Prochlorococcus strain PCC 9511: Combined effects of light and cell cycle, Limnol. Oceanogr., 56, 850–863, 2005.

Cai, W.-J., Hu, X., Huang, W.-J., Murrell, M. C., Lehrter, J. C., Lohrenz, S. E., Chou, W.-C., Zhai, W., Hollibaugh, J. T., Wang, Y., Zhao, P., Guo, X., Gundersen, K., Dai, M., and Gong, G.-C.: Acidi?cation of subsurface coastal waters enhanced by eutrophication, Nature Geosci., 4, 766–770, 2011.

Charette, M. A., Moran, S. B., Pike, S. M., and Smith, J. S.: Investigating the carbon cycle in the Gulf of Maine using the natural tracer thorium 234, J. Geophys. Res., 106, 11553–11579, 2001.

Chen, C.-T. A. and Borges, A. V.: Reconciling opposing views on carbon cycling in the coastal ocean: continental shelves as sinks and near-shore ecosystems as sources of atmospheric CO_2, Deep-Sea Res. II, 56, 578–590, 2009.

Ciais, P., Borges, A. V., Abril, G., Meybeck, M., Folberth, G., Hauglustaine, D., and Janssens, I. A.: The impact of lateral carbon fluxes on the European carbon balance, Biogeosciences, 5, 1259–1271, doi:10.5194/bg-5-1259-2008, 2008.

Copin-Montegut, C., Begovic, M., and Merlivat, L.: Variability of the partial pressure of CO_2 on diel to annual time scales in the Northwestern Mediterranean Sea, Mar. Chem., 85, 169–189, 2004.

Cullen, J. J., Lewis, M., Davis, C. O., and Barber, R.: Photosynthetic characteristics and estimated growth rates indicate grazing is the proximate control of primary production in the Equatorial Pacific, J. Geophys. Res., 97, 639–655, 1992.

Dall'Olmo, G., Boss, E., Behrenfeld, M. J., Westberry, T. K., Courties, C., Prieur, L., Pujo-Pay, M., Hardman-Mountford, N., and Moutin, T.: Inferring phytoplankton carbon and ecophysiological rates from diel cycles of spectral particulate beam-attenuation coefficient, Biogeosciences, 8, 3423–3439, doi:10.5194/bg-8-3423-2011, 2011.

Dickson, A. G. and Millero, F. J.: A comparison of the equilibrium constants for the dissociation of carbonic acid in seawater media, Deep Sea Res., 34, 1733–1743, doi:10.1016/0198-0149(87)90021-5, 1987.

Doney, S. C., Mahowald, N., Lima, I., Feely, R. A., Mackenzie, F. T., Lamarque, J.-F., and Rasch, P. J.: Impact of anthropogenic atmospheric nitrogen and sulphur deposition on ocean acidi?cation and the inorganic carbon system, P. Natl. Acad. Sci., 104, 14580–14585, 2007.

Eppley, R. W., Holm-Hansen, O., and Strickland, J. D. H.: Some observations on the vertical migration of dinoflagellates, J. Phycol., 4, 333–340, doi:10.1111/j.1529-8817.1968.tb04704.x, 1968.

Forget, M. H., Fuentes-Yaco, C., Sathyendranath, S., Platt, T., Pommier, J., and Devred, E.: Computation of primary production from remote sensing of ocean colour at the northwestern Atlantic C-SOLAS Lagrangian site, Mar. Ecol. Prog. Ser., 352, 27–38, 2007.

Gardner, W. D., Walsh, I. D., and Richardson, M. J.: Biophysical forcing of particle production and distribution during a spring bloom in the North Atlantic, Deep Sea Res. Part II: Topical Studies in Oceanography, 40, 171–195, doi:10.1016/0967-0645(93)90012-c, 1993.

Gernez, P., Antoine, D., and Huot, Y.: Diel cycles of the particulate beam attenuation coefficient under varying trophic conditions in the northwestern Mediterranean Sea: Observations and model-

ing, Limnol. Oceanogr., 56, 17–36, 2011.

Greenan, B. J. W., Petrie, B. D., Harrison, W. G., and Oakey, N. S.: Are the spring and fall blooms on the Scotian Shelf related to short-term physical events?, Cont. Shelf Res., 24, 603–625, 2004.

Greenan, B. J. W., Petrie, B. D., Harrison, W. G., and Strain, P. M.: The Onset and Evolution of a Spring Bloom on the Scotian Shelf, Limnol. Oceanogr., 53, 1759–1775, 2008.

Hall, N. S. and Paerl, H. W.: Vertical migration patterns of phytoflagellates in relation to light and nutrient availability in a shallow microtidal estuary, Marine Ecology Progress Series, 425, 1–19, doi:10.3354/meps09031, 2011.

Harrison, G., Johnson, C., Spry, G., Pauley, K., Maass, H., Kennedy, M., Porter, C., and Soukhovtsev, V.: Optical, chemical and biological oceanographic conditions in the Maritimes region in 2007, Canadian Science Advisory Secretariat, Department of Fisheries and Oceans, 2008.

Hood, E. M. and Merlivat, L.: Annual to interannual variations of fCO2 in the northwestern Mediterranean Sea: results from hourly measurements made by CARIOCA buoys, 1995–1997, J. Mar. Res., 59, 113–131, 2001.

Hood, E. M., Wanninkhof, R., and Merlivat, L.: Short timescale variations of fCO_2 in a North Atlantic warm-core eddy: Results from the Gas-Ex 98 carbon interface ocean atmosphere (CARlOCA) buoy data, J. Geophys Res., 106, 2561–2575, 2001.

Lefèvre, N. and Merlivat, L.: Carbon and oxygen net community production in the eastern tropical Atlantic estimated from a moored buoy, Global Biogeochem. Cycles, 26, GB1009, doi:10.1029/2010GB004018, 2012.

Lefèvre, N., Guillot, A., Beaumont, L., and Danguy, T.: Variability of fCO_2 in the Eastern Tropical Atlantic from a moored buoy, J. Geophys. Res., 113, C01015, doi:10.1029/2007/JC004146, 2008.

Leinweber, A., Gruber, N., Frenzel, H., Friederich, G. R., and Chavez, F. P.: Diurnal carbon cycling in the surface ocean and lower atmosphere of Santa Monica Bay, California, Geophys. Res. Lett., 36, L08601, doi:10.1029/2008GL037018, 2009.

Lewis, E. and Wallace, D. W. R.: Program developed for CO2 system calculations, Rep. ORNL/CDIAC-105, Carbon Dioxide Inf. Anal. Cent., Oak Ridge Natl. Lab., US Dep. of Energy, Oak Ridge, Tenn., 1998.

Marra, J.: Analysis of diel variability in chlorophyll fluorescence, J. Mar. Res., 55, 767–784, doi:10.1357/0022240973224274, 1997.

MacIntyre, J. G., Cullen, J. J., and Cembella, A. D.: Vertical migration, nutrition and toxicity in the dinoflagellate Alexandrium tamarense, Marine Ecology Progress Series, 148, 201–216, doi:10.3354/meps148201, 1997.

Nahorniak, J. S., Abbott, M. R., Letelier, R. M., and Pegau, W. S. C.: Analysis of a method to estimate chlorophyll-a concentration from irradiance measurements at varying depths, J. Atmos. Ocean. Technol., 18, 2063–2073, 2001.

Omar, A. M., Olsen, A., Johannessen, T., Hoppema, M., Thomas, H., and Borges, A. V.: Spatiotemporal variations of fCO_2 in the North Sea, Ocean Sci., 6, 77–89, doi:10.5194/os-6-77-2010, 2010.

Schiettecatte, L.-S., Gazeau, F., van der Zee, C., Brion, N., and Borges, A. V.: Time series of the partial pressure of carbon dioxide (2001–2004) and preliminary inorganic carbon budget in the Scheldt plume (Belgian coast waters), Geochem. Geophys. Geosys., 7, Q06009, doi:10.1029/2005GC001161, 2006.

Shadwick, E. H., Thomas, H., Comeau, A., Craig, S. E., Hunt, C. W., and Salisbury, J. E.: Air-Sea CO_2 fluxes on the Scotian Shelf: seasonal to multi-annual variability, Biogeosciences, 7, 3851–3867, doi:10.5194/bg-7-3851-2010, 2010.

Shadwick, E. H., Thomas, H., Azetsu-Scott, K., Greenan, B. J. W., Head, E., and Horne, E.: Seasonal variability of dissolved inorganic carbon and surface water pCO_2 in the Scotian Shelf region of the Northwestern Atlantic, Mar. Chem., 124, 23–37, 2011a.

Shadwick, E. H., Thomas, H., Prowe, A. E. F., and Horne, E.: Spatio-temporal variability of the CO_2 system on the Scotian Shelf, Biogeosciences Discuss., 8, 12013–12050, doi:10.5194/bgd-8-12013-2011, 2011b.

Shadwick, E. H. and Thomas, H.: Carbon Dioxide in the Coastal Ocean: A Case Study in the Scotian Shelf Region, in: Ocean Year Book, 25, edited by: Chircop, A., Coffen-Smout, S., and McConnell, M., Martinus Nijhoff, Leiden/Boston, 171–204, 2011.

Siegel, D. A., Dickey, T. D., Washburn, L., Hamilton, M. K., and Mitchell, B. G.: Optical determination of particulate abundance and production variations in the oligotrophic ocean, Deep-Sea Res. I, 36, 211–222, 1989.

Stramska, M. and Dickey, T. D.: Variability of bio-optical properties of the upper ocean associated with diel cycles in phytoplankton population, J. Geophys. Res., 97, 17873–17887, 1992.

Thomas, H. and Schneider, B.: The seasonal cycle of carbon dioxide in Baltic Sea surface waters, J. Mar. Sys., 22, 53–67, 1999.

Thomas, H., Bozec, Y., Elkalay, K., and de Baar, H. J. W.: Enhanced open ocean storage of CO_2 from shelf sea pumping, Science, 304, 5673, 1005–1008, 2004.

Thomas, H., Unger, D., Zhang, J., Liu, K.-K., and Shadwick, E. H.: Biogeochemical cycling in semi-enclosed marine systems and continental margins, in: Watersheds, Bays and Bounded Seas (SCOPE No. 70), edited by: Urban, E., Sundby, B., Malanotte-Rizzoli, P., and Melillo, J., Island Press, Washington, D.C., 169–190, 2008.

Thomas, H., Schiettecatte, L.-S., Suykens, K., Koné, Y. J. M., Shadwick, E. H., Prowe, A. E. F., Bozec, Y., de Baar, H. J. W., and Borges, A. V.: Enhanced ocean carbon storage from anaerobic alkalinity generation in coastal sediments, Biogeosciences, 6, 267–274, doi:10.5194/bg-6-267-2009, 2009.

Umoh, J. U. and Thompson, K. R.: Surface heat flux, horizontal advection, and the seasonal evolution of water temperature on the Scotian Shelf, J. Geophys. Res., 99, 403–420, 1994.

Urrego-Blanco, J. and Sheng, J.: Interannual variability of circulation and hydrography over the Eastern Canadian Continental Shelf, Atmosphere-Ocean, 50, in press, doi:10.1080/07055900.2012.680430, 2012.

Vandemark, D., Salisbury, J. E., Hunt, C. W., Shellito, S., and Irish, J.: Temporal and spatial dynamics of CO_2 air-sea flux in the Gulf of Maine, J. Geophys. Res., 116, C01012, doi:10.1029/2010JC006408, 2011.